

## Reduction Behaviors of Nitric Oxides on Copper-decorated Mesoporous Molecular Sieves

Ki-Sook Cho, Byung-Joo Kim,<sup>†</sup> Seok Kim,<sup>‡</sup> Sung-Hyun Kim, and Soo-Jin Park<sup>§,\*</sup>

*Environment Systems Engineering, Korea University, Seoul 136-701, Korea*

<sup>†</sup>*Nano Material Research Dept., Jeonju Institute of Machinery and Carbon Composites, Jeonju 561-844, Korea*

<sup>‡</sup>*Dept. of Chemical and Biochemical Engineering, Pusan National Univ., Pusan 609-735, Korea*

<sup>§</sup>*Dept. of Chemistry, Inha Univ., Incheon 402-751, Korea. \*E-mail: sjpark@inha.ac.kr*

*Received July 15, 2009, Accepted November 24, 2009*

In this study, NO reduction behaviors of copper-loaded mesoporous molecular sieves (Cu/MCM-41) have been investigated. The Cu loading on MCM-41 surfaces was accomplished by a chemical reduction method with different Cu contents (5, 10, 20, and 40%). N<sub>2</sub>/77 K adsorption isotherm characteristics, including the specific surface area and pore volume, were studied by BET's equation. NO reduction behaviors were confirmed by a gas chromatography. From the experimental results, the Cu loading amount on MCM-41 led to the increase of NO reduction efficiency in spite of decreasing the specific surface area of catalysts. This result indicates that highly ordered porous structure in the MCM-41 and the presence of active metal particles lead the synergistical NO reduction reactions due to the increase in adsorption energy of MCM-41 surfaces by the Cu particles.

**Key Words:** NO reduction, Mesoporous molecular sieve, Textural properties

### Introduction

Air pollution has been aggravated by four developments: increasing traffic, urban growth, rapid economic development, and industrialization. Air pollution threatens the health of human beings and other life on our planet.<sup>1</sup> Increasingly stringent regulation of air pollution emission requires further investigations on suppressing emission of harmful matters from high temperature industrial processes. It has been long recognized that nitrogen monoxide, NO is one of the harmful air pollutants in the processes. Nitric oxide in the air can convert to nitric acid, which has been implicated in acid rain. Furthermore, both NO and NO<sub>2</sub> participate in ozone layer depletion. Nitric oxide is a small highly diffusible gas and a ubiquitous bioactive molecule.<sup>2,3</sup>

As a thermodynamic perspective, NO is unstable with respect to O<sub>2</sub> and N<sub>2</sub>, although this conversion is very slow at ambient temperatures in the absence of a catalyst because the heat of formation of NO is endothermic. However, the use of internal combustion engines has drastically increased the presence of nitric oxide in the environment. To overcome these problems, some researchers have reported NO reduction technology using metals supported on activated carbons (ACs) or activated carbon fibers (ACFs) by impregnation, metal plating, deposition, and so on.<sup>4,5</sup>

However, porous carbons above mentioned have micropores ( $r < 2$  nm) richly, meaning that the specific surface area and the pore volume of the support can be severely reduced after metal loading by the blocking or filling of pores. So, it is thinkable that the support having mesopores richly can be suitable for metal loading in order to avoid severe pore blocking.

MCM-41, a member of the newly discovered mesoporous molecular sieves M41S family, processes a regular hexagonal array of uniform pore openings with a broad spectrum of pore diameters between 15 and 100 Å.<sup>6-9</sup> This means that proper MCM-41 samples can be designed for a specified toxic gas by

changing pore diameters. Through the control of preparation conditions, such as a template, a reaction temperature, time,<sup>10</sup> and pH value,<sup>11</sup> high quality MCM-41 materials can be obtained with the properties such as high specific surface area, large pore volume, and ordered pore size.<sup>12</sup> Moreover, the MCM-41 are mainly composed of SiO<sub>2</sub> molecules, indicating that the surface polarity can be high enough to have good chemical affinity with toxic polar gases, such as NO<sub>x</sub> or SO<sub>x</sub>.

These materials are promising as catalytic supports for materials such as metal oxides and organometallic compounds because of their large surface area and ordered mesoporous structure. The synthesis of mesoporous catalysts with redox properties is carried out by introducing transition metals such as Ti, V, Zr, and Cr in the silica.

Supported Cu catalysts are known as interesting materials because of the low cost of Cu and the advantageous catalytic properties of Cu-containing catalysts for various classes of reaction.<sup>13</sup>

The objective of the present work is to investigate the surface properties and textural properties of Cu/MCM-41, to discuss the NO reduction behaviors of Cu/MCM-41 with different Cu content, and to evaluate the possibility of MCM-41 as a filter media for toxic gases.

### Experimental

**Sample preparation.** To prepare MCM-41, fumed silica was added to cetyltrimethylammonium chloride solution (25 wt %, Aldrich) at certain mixing ratio and pH value of 13. After drying, the as-synthesized samples were heated in the stream of air for 6 h at 823K. For the observation of MCM structures, a TEM was employed. The Cu/MCM-41 samples were prepared by stirring MCM-41 for 1 h at room temperature and for 1 h at 323 K with 0.023 M solution of Cu(II) acetylacetonate in chloroform, and then the chloroform was evaporated. A Cu loading was con-

trolled by using Cu(II) acetylacetonate solution with initial concentrations of 5, 10, 20, and 40% and named as 5%-CM, 10%-CM, 20%-CM, and 40%-CM.

**Textural properties.** Nitrogen adsorption isotherms were measured by using an ASAP 2010 (Micromeritics) at 77 K. Prior to each analysis, the samples were outgassed at 573 K for 12 h to obtain a residual pressure of less than  $10^{-3}$  torr. The amount of nitrogen adsorbed, which was used to calculate specific surface area and pore volume was investigated by BET's equation<sup>14</sup> and Boer's *t*-plot method.<sup>15</sup> Total pore volume was estimated to be the liquid volume of nitrogen at a relative pressure of about 0.995.<sup>16,17</sup>

**NO reduction test.** For the present experiments, a gas chromatograph (DS-6200 model, Donam Co.) with a thermal conductivity detector was used to measure NO conversion of the Cu/MCM-41. Reactor temperature was sustained constantly at 500 °C using a PID temperature controller (UP-350, Yokogawa), and the gas flow rate was maintained at 15 mL/min by a mass flow controller (GMC 1000, MKS). All samples were heated under a helium purge at 150 °C for 1 h to remove residual H<sub>2</sub>O before NO conversion test. The NO conversion was determined from the concentration of NO at the outlet reactor. Prior to each analysis, NO standard curve was gained by using the 300, 600, and 1000 ppm NO gas.

## Results and Discussion

**Microstructures.** The small angle XRD patterns of the MCM-41 with and without Cu loading were shown in Figure 1. A major peak at  $2\theta = 2^\circ$  (100) along with three small peaks was observed due to the (110), (200), and (210) plane reflection lines.<sup>6,7</sup> These three reflection lines are generally indexed for the hexagonal unit cell as seen in the TEM image. In case of the Cu/MCM-41 sample, three small peaks mentioned above were not clearly observed. This result indicates that Cu particles can be intercalated into the hexagonal unit cells and affect the changes of reflection lines, resulting in the decrease of typical MCM-41 peaks.

**Surface properties.** Figure 2 shows FT-IR spectra of the MCM-41 and Cu/MCM-41 synthesized. Two strong adsorption bands at 780 and 960  $\text{cm}^{-1}$  suggested that the Si-O-Si and Si-OH structures were found. It was also found that the bands at 960  $\text{cm}^{-1}$  and 1000–1100  $\text{cm}^{-1}$  of the Cu/MCM-41 decreased with Cu loading probably due to the incorporation of Cu particles into the MCM framework. In case of two adsorption bands observed at 1580 and 1630  $\text{cm}^{-1}$ , a Cu complex can be localized in the extra-framework position, to give rise to an intense band at 1630  $\text{cm}^{-1}$  and a small one at 1580  $\text{cm}^{-1}$ .

**Textural properties.** Nitrogen adsorption isotherms of the MCM-41 before and after Cu loading were shown in Figure 3. All of the specimens were approximately the Type IV isotherms showing typical ones according to the IUPAC's classification.<sup>16</sup> A round knee, which indicated the capillary condensation (mesopore filling),<sup>18,19</sup> was observed at  $P/P_0 = 0.29 - 0.37$  in the isotherm of Cu/MCM-41 compared to that of the MCM-41 (at  $P/P_0 = 0.32 - 0.39$ ). It can be explained that the mesopore distribution was shifted to low relative pressure after Cu loading, because Cu particles affected the pore narrowing or blocking of

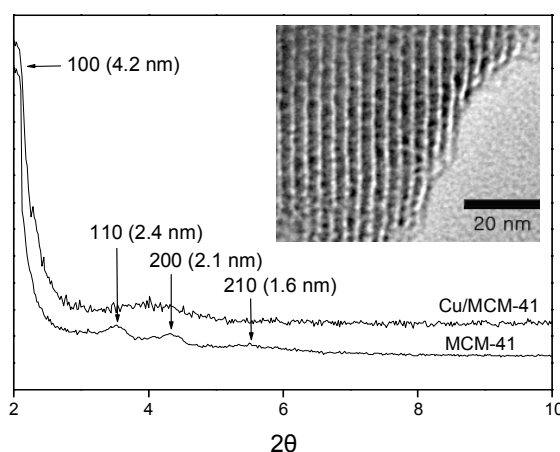


**Figure 1.** TEM image and small angle XRD patterns of the MCM-41 and Cu/MCM-41.

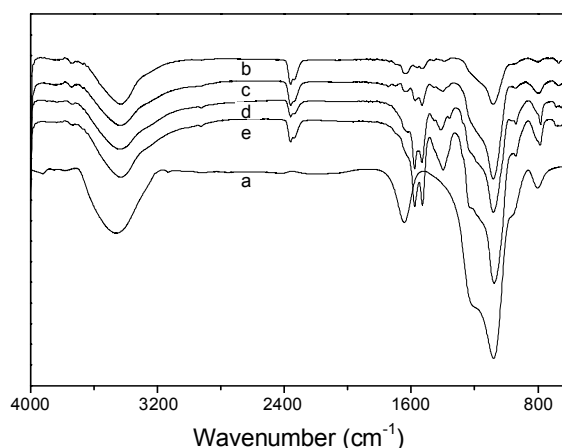


**Figure 2.** FT-IR spectra of the MCM-41 and Cu/MCM-41 as a function of Cu content: (a) MCM-41, (b) 5%-CM, (c) 10%-CM, (d) 20%-CM, (e) 40%-CM.

the mesopores in the MCM-41.

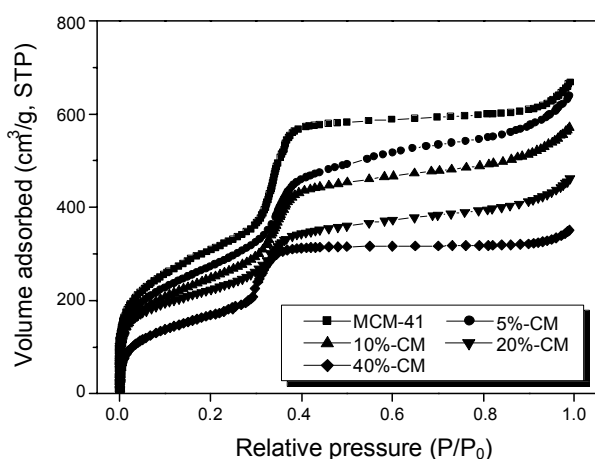
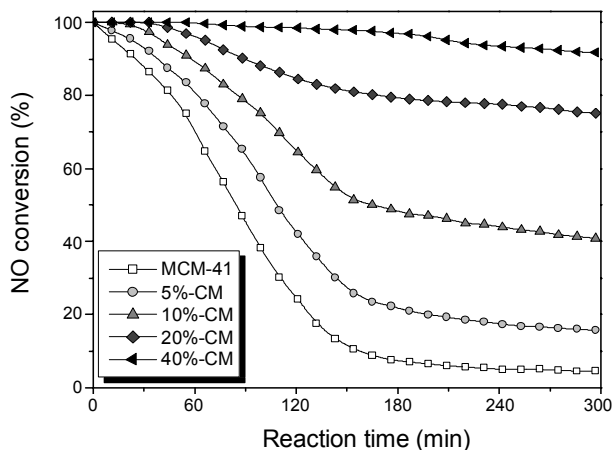
The specific surface areas, pore volumes, total pore volumes, and average pore diameters of the MCM-41 and Cu/MCM-41 are listed in Table 1. It can be seen that the MCM-41 possesses a high specific surface area of 831  $\text{m}^2/\text{g}$  and a large pore volume of 1.034  $\text{cm}^3/\text{g}$ . Textural properties including the specific surface area and the pore volume are somewhat reduced due to the filling or blocking of pores. In addition, the average pore diameter was decreased slightly with Cu loading on the MCM-41. This result probably has a close relation with the shifting of mesopore region in Figure 3.

However, these decrease in pore volume after metal loading is much less than that of carbonaceous support.<sup>2,3,5</sup> As mentioned in the introduction, carbonaceous support have micropore richly, so severe pore blocking must happen. But MCM-41 supports have mesopore mainly, resulting in remarkably less blocked pore volumes.

Moreover, the pore structure of the MCM-41 is highly ordered like tunnels. This result indicates that NO molecules can be easier to reach active metal surfaces in the tunnel-like pores than that of the active carbons which have complex pore struc-

**Table 1.** Textural Properties of the MCM-41 and Cu/MCM-41 as a Function of Metal Content

	MCM-41	5%-CM	10%-CM	20%-CM	40%-CM
Specific surface area (m <sup>2</sup> ·g <sup>-1</sup> )	831	740	670	540	455
Micropore volume (cm <sup>3</sup> ·g <sup>-1</sup> )	0.833	0.667	0.614	0.504	0.409
Total pore volume (cm <sup>3</sup> ·g <sup>-1</sup> )	1.034	0.988	0.884	0.637	0.588
Average pore diameter (Å)	26.9	26.7	26.7	26.5	26.3

**Figure 3.** N<sub>2</sub>/77K adsorption isotherms of the MCM-41 and Cu/MCM-41 as a function of Cu content.**Figure 4.** NO conversion by the MCM-41 and Cu/MCM-41 as a function of Cu content.

ture. Normally activated carbons have macropores, mesopores, and micropores. The adsorption of NO gas is occurred at meso- and micropores, but the complex pore structures and blocking of pores by metal loading can severely decrease the NO reduction ability of the catalyst. The Cu/MCM-41 sample in this work can be free of this problem due to its tunnel-like mesopore structure.

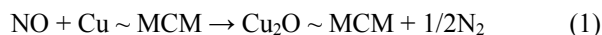
**NO reduction behaviors.** NO reduction behaviors of Cu supported on the MCM-41 samples measured at 500 °C were shown in Figure 4. As a result, the MCM-41 sample had low activity, whereas the Cu/MCM-41 samples had high reduction activity. Also, it could be seen that the NO conversion with the MCM-41

drastically decreased within a few hours, and it reached about 8% after 100 min on stream. However, the NO removal capacities of the Cu/MCM-41 at 500 °C were increased with increasing the Cu content compared to that of MCM-41. The Cu/MCM-41 samples showed NO conversions of about 16, 44, 77, and 89% after 300 min on stream according to the Cu contents of 5, 10, 20, and 40%, respectively. The capacities of 40%-Cu/MCM-41 were kept on removing NO completely for 3 h. Meanwhile, the NO conversion on the MCM-41 was rapidly decreased by 100 min. These results clearly indicated that the Cu loading was effective method in order to enhance the NO reduction capability of MCM-41.

However, several literatures<sup>2,3,5</sup> have reported that excessive metal loading normally decreased total reaction sites, resulting the decrease in NO reduction ability of the samples.

According to our previous work,<sup>20</sup> we revealed that the carbon support didn't chemically adsorb NO gases during the reaction. However, the active metals were oxidized, then were dramatically deoxidized, and finally exhausted N<sub>2</sub> and O<sub>2</sub> gases as confirmed in a gas chromatography.

Similar reaction can occur in the Cu/MCM-41 and NO system as equation (1) and (2).



So, total reaction can be concluded that NO gases are firstly physic-adsorbed on MCM-41 samples and move to active metal surfaces. And they were chemically reacted and produce N<sub>2</sub> and O<sub>2</sub> gases on Cu/MCM-41 surfaces.

## Conclusions

In this work, NO reduction behaviors of Cu/MCM-41 were investigated as a function of Cu content. From the work, the Cu/MCM-41 samples show NO conversion of about 16, 44, 77, and 89% after 300 min on stream according to the various Cu contents of 5, 10, 20, and 40% though the specific surface areas and the pore volumes of the samples decreased along with the increase of Cu loading. This result means that the Cu content on the Cu/MCM-41 plays an important role in improving the NO reduction efficiency, due to the reaction between metallic Cu of the Cu/MCM-41 and NO gas.

## References

- Calvert, S.; Englund, H. M. *Handbook of Air Pollution Technology*; John Wiley & Sons: New York, 1984.

2. Park, S. J.; Kim, B. J. *J. Colloid Interface Sci.* **2005**, *282*, 124.
  3. Park, S. J.; Kim, B. J. *J. Colloid Interface Sci.* **2005**, *292*, 493.
  4. Kim, B. J.; Lee, Y. S.; Park, S. J. *J. Colloid Interface Sci.* **2008**, *318*, 530.
  5. Kim, B. J.; Park, S. J. *J. Colloid Interface Sci.* **2008**, *325*, 121.
  6. Hu, X.; Lei, L.; Chu, H. P.; Yue, P. L. *Carbon* **1999**, *37*, 631.
  7. Ryoo, R.; Ko, C. H.; Park, I. S. *Chem. Commun.* **1999**, *15*, 1413.
  8. Kim, J.; Choi, M.; Ryoo, R. *Bull. Korean Chem. Soc.* **2008**, *29*, 413.
  9. Park, S. J.; Im, S. H. *Bull. Korean Chem. Soc.* **2008**, *29*, 777.
  10. Chen, Y.; Ciuparu, D.; Lim, S.; Yang, Y.; Haller, G. L.; Pfefferle, L. *J. Catal.* **2004**, *226*, 351.
  11. Vidya, K.; Gupta, N. M.; Selvam, P. *Mater. Res. Bull.* **2004**, *39*, 2035.
  12. Zhao, X. S.; Lu, G. Q.; Millar, G. J. *Ind. Eng. Chem. Res.* **1996**, *35*, 2075.
  13. Hadjiivanov, K.; Tsoncheva, T.; Dimitrov, M.; Minchev, C.; Knozinger, H. *Appl. Catal. A: General* **2003**, *241*, 331.
  14. Brunauer, S.; Emmett, P. H.; Teller, E. *J. Am. Chem. Soc.* **1938**, *60*, 309.
  15. de Boer, J. H.; Linsen, B. G.; Plas, T.; Zonder, G. J. *J. Catal.* **1965**, *4*, 649.
  16. Boehm, H. P. *Adv. Catal.* **1966**, *16*, 179.
  17. Dubinin, M. M.; Radushkevich, L. V. *Doklady Akad. Nauk SSSR.* **1947**, *55*, 331.
  18. Sing, K. S. W.; Everett, D. H.; Haul, R. A. W.; Moscou, L.; Pierotti, R. A.; Rouquol, J.; Siemieniewska, T. *Pure Appl. Chem.* **1985**, *57*, 603.
  19. Li, Z.; Gao, L. *J. Phys. Chem. Solids* **2003**, *64*, 223.
  20. Park, S. J.; Jang, Y. S.; Kawasaki, J. *Hwahak Konghak* **2002**, *40*, 664.
-